JOURNAL OF CATALYSIS 3, 229–238 (1964)

High-Purity Alumina I.
The Nature of Its Surface Acid Sites and Its Activity in Some Hydrocarbon Conversion Reactions

SHAO E. TUNG AND EDWARD MCININCH

From the Catalysis Research Laboratory, Central Research Division, Continental Oil Company, Ponca City, Oklahoma

Received November 27, 1963

The activities of high-purity alumina and those of silica-alumina were compared for four types of hydrocarbon conversion reactions. It was shown that high-purity alumina possesses fairly good activity for butene-1 isomerization but relatively poor activity for propylene polymerization at 195°C and for cumene cracking and hexene cracking below 400°C. Above 400°C, high-purity alumina has good cracking activity.

These observations are explained by assuming the presence of two types of acid sites on alumina surfaces—the Lewis acid sites and the *passive Bronsted acid sites.* The passivity of Bronsted acids is assumed to arise from the combination of protons with cationic vacancies on the alumina surface. The dissociation energy of these proton–vacancy combinations is estimated to be higher than 0.06 ev.

INTRODUCTION

High-purity alumina has been used as a base for platinum catalysts in petroleum refining for a number of years. However, it is only since 1960 (*1*), that its catalytic properties have been systematically elucidated and documented. It is now well established that alumina, when sufficiently pure, is acidic and its acidity is generally characterized as being of the Lewis type. Very little has yet been said about the presence or absence of Bronsted acidity on the alumina surface. Since, in the case of silica-alumina, a number of surface reactions with carbonium ion mechanisms are known to be promoted by Bronsted acids, whether the alumina surface can hold Bronsted acidity is expected to be significantly related to its catalytic activity.

In order to gain some insight into this and related problems, we have studied a number of hydrocarbon conversion reactions with alumina as catalyst. These experiments were carried out concurrently with parallel experiments with silica-alumina and with pure silica. The results of our study of four types of reactions, namely, propylene polymerization at 195°C, cumene cracking, hexene-1 cracking, and butene-1 isomerization are reported here.

Emphasis in this paper lies on the characteristics of acid sites on alumina surfaces as deduced from its catalytic activity. Mechanisms of the reactions will be discussed in later communications.

EXPERIMENTAL

Materials

Three kinds of alumina, one silica-alumina, and one pure silica, were used as catalysts. Alumina A is the high-purity variety, prepared as described below. Alumina B is less pure. Alumina C is a commercial variety, Kaiser 101. The silica-alumina catalyst chosen was American Cyanamid's Aerocat, containing approximately 13% alumina. The silica was prepared by hydrolyzing distillation-purified tetraethoxysilane with distilled water.

The chemicals used were obtained from

the following sources: cumene, Phillips' research grade, 99.99+ mole % purity; hexene-1, Phillips' pure grade, 99 mole % purity; butene-1, Phillips' instrumental grade, 99 mole % purity; and propylene, Phillips' C.P. grade, 99.0 mole % purity. The propylene was further purified by passing it through a wash train containing aluminum triethyl to remove any oxygen-bearing compounds before use. Helium gas used in the experiments was dried by passing it through a silica gel column.

Procedures

(A) Alumina preparation. The hydroxide of alumina A was prepared by hydrolyzing alumina alcoholate* with distilled water (sodium content 0.18 ppm) and of alumina B with tap water (sodium content 108 ppm). The alcoholate used had an average chain length of 12 carbon atoms and contained approximately 6% aluminum. The hydroxides were dried at 90°C in a vacuum oven (13 mm Hg) for 24 hr. The dried solids had a water content of 50% and a total volatile matter of 72%. Under X-ray examination, these hydroxides gave an α-monohydrate diffraction pattern. Some of the crystals may be pseudo α-monohydrate (*3*), since upon calcination (650°C, 4 hr) the material yielded some eta alumina. The calcined material has a crystallite size ranging from 30–50 Å by X-ray measurement and a BET surface area of around 280 m^2/g.

(B) Propylene polymerization. The polymerization was carried out statically in a Pyrex reactor (total volume 450 ml) provided with a magnetic stirrer. Five grams of catalyst was weighed into the reactor and calcined in air *in situ* at 500°C for an hour. The reactor was then cooled, immersed in a boiling ethylene glycol bath (b.p. 195°C), evacuated, and charged with propylene gas to 600 mm Hg pressure above atmospheric. The pressure drop was then measured at intervals over a period of 3 hr.

(C) Cumene cracking. The cracking was performed by passing cumene over a catalyst bed (0.8 g catalyst) packed in a Vycor glass microreactor (12 mm diameter). The reactor was heated by a vertical furnace, and the temperature of the bed was controlled to ±3°C. The cumene was placed in a saturator maintained at 0°C and was carried over the reactor bed by a gentle dried helium gas stream (31 ml/min).

All catalysts were precalcined in air at 650°C for 4 hr before being placed in the reactor. They were then heated *in situ* at 550°C under a 50 ml/min helium stream for 1 hr. When the catalyst was properly cooled to the lowest temperature level covered in the study, cumene was admitted. The product gas from the reactor was led through a gas sample loop (5 ml) which could be switched from time to time into a vapor fractometer for analysis. When the product gas composition became reproducible, the reactor was heated to the next higher temperature level, and the study was repeated at that level.

Two chromatographic columns, a 15-ft Resoflex R-728 on 42/60 Tyler support column and a 2-ft 100/200 silica gel column, were arranged in series. The aliphatic peaks were first allowed to travel through both columns and come out the silica gel column in succession. After the last aliphatic peak was registered, the silica gel column was switched out. The conditions of analysis (120°C, 12 psig, and helium flow rate 35 ml/min) were adjusted so that the aromatic peaks would next come through the Resoflex column and were registered by the detector directly. All the peaks were registered by a thermoconductivity cell.

(D) Hexene-1 cracking. The same microreactor was used but in this case hexene was fed in as liquid. Catalysts used (2 g) were also pretreated as in cumene cracking. The liquid hexene was fed into the reactor tube by a syringe-type displacement pump at a rate of 0.3 ml/min. Temperature levels studied include 380°, 425°, 470°, 500°, and 520°C. A new catalyst sample was used for each temperature level studied.

---

* From Continental "ALFOL" alcohol plant (*2*).

The liquid products were removed by a water condenser. The gaseous products were collected over water. Rates of liquid and gaseous product accumulation were separately recorded.

Analysis of the gaseous product was carried out in a vapor fractometer. Three samples of the same product gas were analyzed with different column–detector combinations. The first sample was analyzed with a 15-ft HMPA (hexamethyl phosphoramid) on 60/80 G.C. 22 column (28 ± 2°C, 18 psig, nitrogen flow rate 25 ml/min) and a hydrogen flame detector. This gave a general product pattern. To resolve ethane and ethylene, a second sample was analyzed with a 6-ft 100/200 silica gel column (28 ± 2°C, 18 psig, nitrogen flow rate 25 ml/min) and the same hydrogen flame detector. A third sample was sent through a 9-ft 100/200 silica gel column (28 ± 2°C, 29 psig, nitrogen flow rate 55 ml/min) and a thermoconductivity cell to determine hydrogen. Nitrogen, instead of helium, was used as diluent in all these analyses.

(E) Butene-1 isomerization. The same microreactor assembly as in cumene cracking was used. The catalysts were also similarly pretreated. A mixture of 30% butene-1 in helium was used as reactant gas. It was allowed to flow through the catalyst bed (1 g catalyst) at a rate of 12 ml/min. At each temperature level, the reaction was maintained for 50 min to achieve a steady state before the product gas was analyzed. The analysis was performed in a vapor fractometer using a 40-ft $AgNO_3$-benzyl cyanide on 42/60 firebrick column (28 ± 2°C, psig, helium flow 55 ml/min) and a thermoconductivity cell.

RESULTS

Table 1 gives the impurity contents and some physical characteristics of the catalysts used.

The activities of various catalysts in propylene polymerization is plotted in

TABLE 1
VARIOUS CATALYSTS—PHYSICAL PROPERTIES AND IMPURITY CONTENTS

	Alumina A	Alumina B	Alumina C	Silica-alumina	Silica
		Physical properties			
Surface area[a] (m²/g)	280.5	279.2	227.2	266.7	411.8
Crystal Form	Essentially gamma, some eta	Essentially gamma, some eta	Eta and some gamma	Amorphous	Amorphous
Crystallite size (Å)	30.7	42.3	45.3	—	—
		Impurity content[b] *(ppm)*			
Sodium	10	170	3660	144	11
Calcium	10	2000	1000	1000	10
Magnesium	10	200	—	100	10
Iron	75	75	50	505	11
Silicon	40	1000	1000	—	—
Copper	10	10	10	10	10
Nickel	10	10	10	100	10
Chromium	10	10	10	200	10
Tin	10	10	10	10	100
Manganese	—	10	100	10	10
Sulfur	25	—	—	1642	10

[a] By BET nitrogen adsorption.

[b] Sodium was analyzed by flame photometer, iron and sulfur by X-ray fluorescence, and the rest by the emission spectrometer.

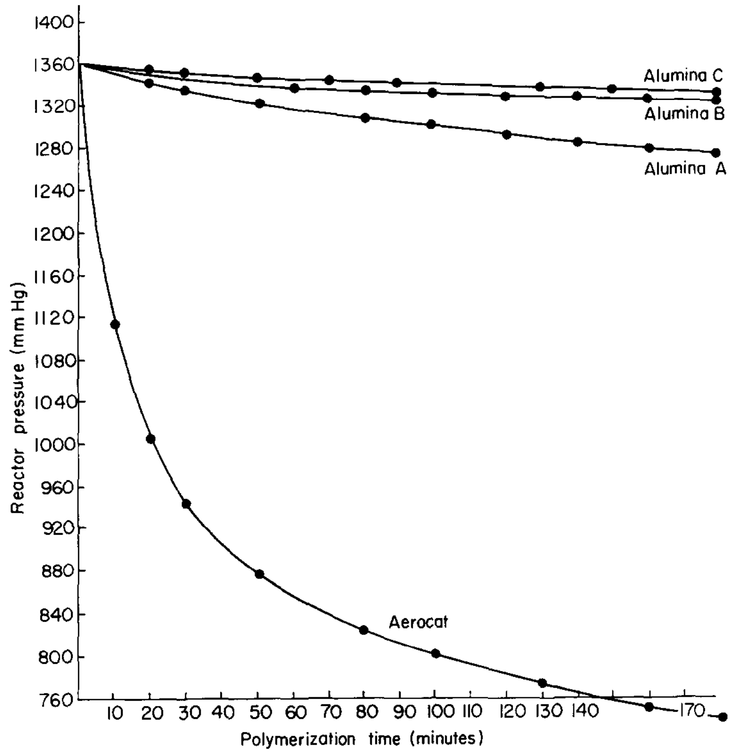

FIG. 1. Rate of propylene polymerization (pressure drop vs polymerization time); polymerization temperature = 195°C.

terms of pressure drop in Fig. 1. None of the aluminas shows much activity in comparison with silica-alumina, although alumina A appears more reactive than the others.

Cumene-cracking rate data are presented in Fig. 2, and some typical product gas compositions are given in Table 2. Cumene can be easily cracked by silica-alumina, while with alumina A the reaction does not start below 400°C. Aluminas B and C and silica exhibit hardly any activity up to the

TABLE 2

TYPICAL PRODUCT GAS COMPOSITION IN CUMENE CRACKING

	Catalyst				
	Aerocat	Alumina A	Alumina B	Alumina C	Silica
Temperature (°C)	350°	500°	500°	500°	500°
Product (Mole %)					
Hydrogen + methane	—	11.0	—	—	—
Ethane + ethylene	—	0.8	—	—	—
Propylene	48.7	11.5	—	—	—
Benzene	48.4	17.5	—	—	—
Toluene	—	2.2	—	—	—
Cumene	2.9	37.0	100	100	100
Stylene	—	9.3	—	—	—
Polyalkylbenzene, etc.	Trace	10.7	—	—	—

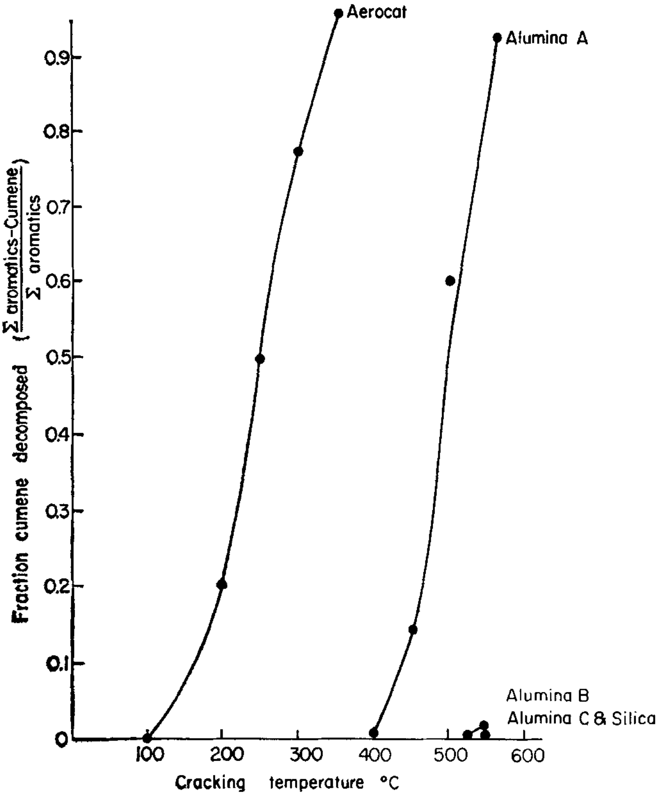

FIG. 2. Rate of cumene cracking.

highest temperature covered (545°C). The product gases from silica-alumina cracking are dominantly propylene and benzene with only trace amounts of polyalkyl benzene present. Alumina A generates more complex product gases, as are shown in Table 2.

The rates of hexene-1 cracking are compared in Figs. 3 and 4. Figure 3 shows that for hexene-1 cracking, silica-alumina is more active than alumina A and that for alumina A, the cracking does not begin below 425°C. The rate of cracking on alumina A is further examined in Fig. 4 where the volume of gas generated per unit volume of feed is plotted against cumulative volume of feed passed through the reactor. Fresh alumina shows a high initial activity, but the rate soon levels off for a certain temperature level of cracking. This plot further shows that hexene cracking does not begin significantly below 400°C.

Representative product gas analyses are given in Table 3. Aerocat gives a typical acid cracking pattern with propylene as the main product. In comparison, the product gas from alumina contains a good deal more hydrogen, more light hydrocarbon gases, but less propylene.

Some of the butene-1 isomerization data are shown in Table 4. In addition, the composition of the isomerization product from alumina A is plotted against equilibrium curves for mixtures of the butene-1, *cis*-butene-2, and *trans*-butene-2 system (*4*) in Fig. 5. This plot brings forth the fact that butene-1 isomerization proceeds in several stages. At lower temperatures, only the double bond shift occurs, and this reaches equilibrium at 200°C. Between 200° and 310°C, this equilibrium prevails. At 310°C, isobutylene starts to form through skeletal isomerization, and the concentration of isobutylene keeps on increasing with temperature until about

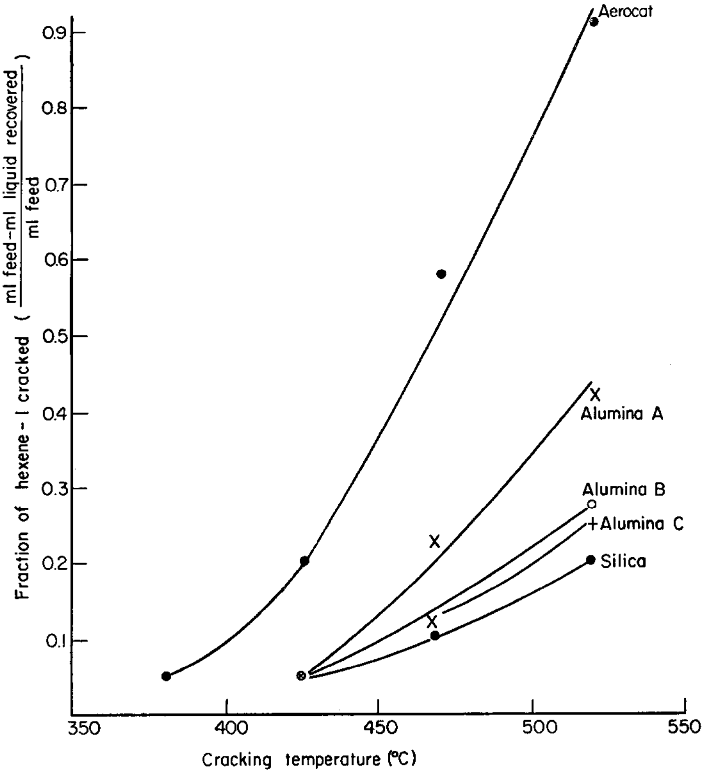

FIG. 3. Rate of hexene-1 cracking.

TABLE 3
TYPICAL PRODUCT GAS COMPOSITION IN HEXENE-1 CRACKING AT 500°C[a]

	Catalyst				
	Aerocat	Alumina A	Alumina B	Alumina C	Silica
Hydrogen	8.2	49.6	60.1	31.4	1.7
Methane	5.1	11.1	12.4	26.6	22.1
Ethane	2.5	2.2	3.6	14.0	13.5
Ethylene	5.6	14.6	11.2	12.5	32.1
Propane	3.9	0.6	0.2	1.5	2.7
Propylene	50.6	9.7	6.5	8.1	20.0
Isobutane	4.1	0.1	—	0.2	—
n-Butane	0.7	—	0.1	0.1	0.3
Isobutylene + butene-1	11.6	9.4	3.5	2.8	3.6
Trans-butene-2	4.3	1.7	0.9	0.9	0.4
Cis-butene-2	3.2	1.0	0.6	0.6	0.3
Butadiene	—	—	0.4	1.5	3.3

[a] Composition in mole per cent.

475°C, where cracking begins. Similar plots can be made for the other catalysts, and Table 5 summarizes some of the information from these plots. In general, silica-alumina is more active than alumina A in promoting double bond shift reactions at

TABLE 4

Product Composition in Butene Isomerization at 470°C[a]

	Catalyst				
	Aerocat	Alumina A	Alumina B	Alumina C	Silica
Hydrogen and methane	0.5	1.6	—	—	—
Ethane	0.1	—	—	—	—
Ethylene	—	—	—	—	—
Propane	—	—	—	—	—
Propylene	7.9	3.1	—	—	—
n-Butane	0.5	—	—	—	—
Isobutane	0.8	—	—	—	—
Butene-1	23.2	20.7	28.0	39.4	87.8
Trans-butene-2	25.8	27.7	39.8	33.5	5.4
Cis-butene-2	20.4	20.8	30.4	27.1	6.8
Isobutylene	20.8	26.1	1.8	—	—
Butadiene	—	—	—	—	—

[a] Composition in mole per cent.

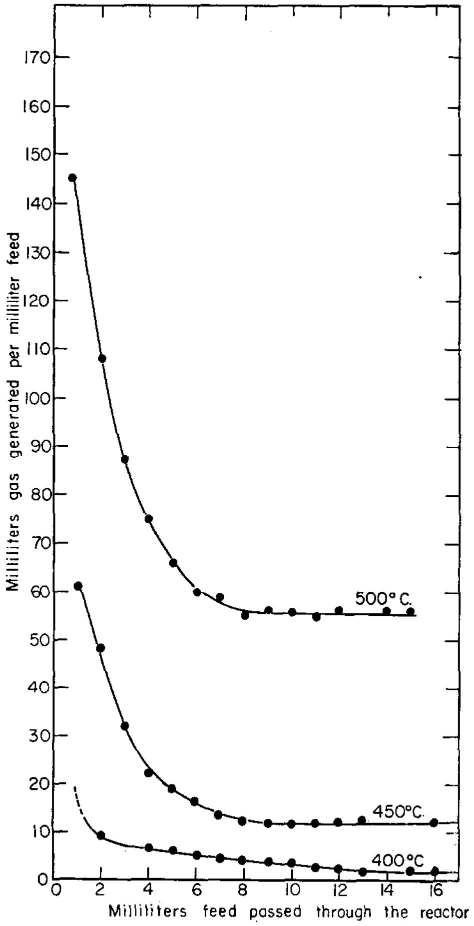

Fig. 4. Rate of hexene-1 cracking (product gas generation).

TABLE 5

Butene-1 Isomerization with Different Catalysts

	Temperature where double bond shift reaches equilibrium (°C)	Temperature where skeletal isomerization begins (°C)
Aerocat	200	310
Alumina A	200	310
Alumina B	270	475
Alumina C	500	545
Silica	—	—

lower temperature levels, although alumina A does possess fairly good activity as is shown by Fig. 5. These double bond shift reactions reach equilibrium at about the same temperature for both alumina A and silica-alumina (Table 5). Furthermore, alumina A seems to yield more isobutylene than silica-alumina before cracking begins. This is shown in Fig. 6. This latter figure also shows that a trace contamination of alumina by impurities is quite detrimental to its isomerization activity. It should be pointed out that the activity of alumina A toward butene isomerization is very sensitive to the conditions of calcination, storage, etc.

Discussion

In contrast to silica-alumina, the activity of alumina toward the hydrocarbon re-

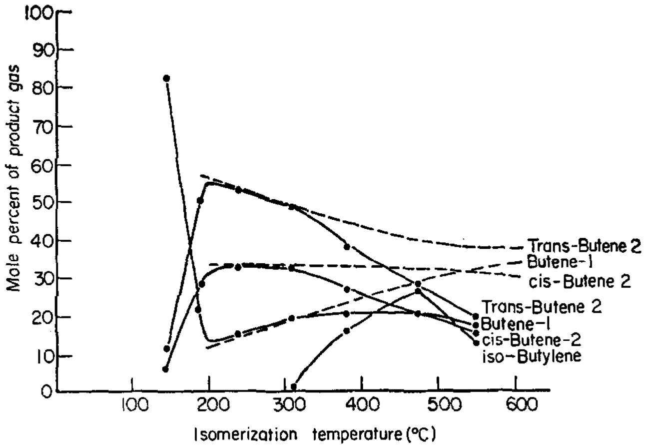

FIG. 5. Composition of butene-1 isomerization product with alumina A. (Dotted lines represent the equilibrium composition in butene-1, *trans*-butene-2, *cis*-butene-2 system—after Voge and May, ref. *5*).

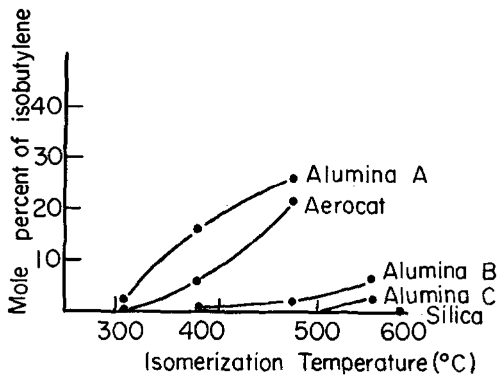

FIG. 6. Isobutylene in the isomerization product.

actions studied may be summarized as follows:

(1) Pure alumina is a relatively poor catalyst for propylene polymerization, cumene cracking, and hexene cracking below 400°C. On the other hand, it does possess fairly good catalytic activity for butene isomerization.

(2) Above 400°C, pure alumina promotes cumene cracking and hexene cracking and its activity increases as temperature increases.*

It seems that the first observation can be best explained by assuming the presence of Lewis acid sites on the alumina surface; below 400°C, the catalytic action of alumina surfaces is essentially attributable to these sites. Upon further assuming that Lewis acid sites can effectively promote butene isomerization but are relatively impotent toward cracking and polymerization, which need Bronsted acids, the observation on alumina activity as summarized in statement (1) becomes understandable.

This latter assumption is seemingly consistent with the works reported by Holm *et al.* (*5*), Hansford (*6*), and Peri (*7*). Holm *et al.*, working with silica-alumina catalysts, demonstrated that a small amount of water on the catalyst surface drastically enhanced the rates of propylene polymerization. A similar dependence on water was reported by Hansford for butane cracking on silica-alumina. The importance of Bronsted acids to the polymerization and cracking reactions has been discussed by these authors. On the other hand, Peri, from his infrared study, concluded that butene isomerization on alumina takes place on Lewis acid sites.

The second observation, namely, the activity of alumina toward cracking reactions above 400°C, can be best explained, we believe, by assuming the presence of

* Alumina also generates more hydrogen gas in its cracking product than silica-alumina. This is due to the presence of dehydrogenation centers on the alumina surfaces and will not be discussed in the present communication.

passive Bronsted acids on the alumina surface in addition to the Lewis acids. This passivity is assumed to arise from the combination of protons with cationic vacancies. By further assignment of dissociation energy values of 0.06 ev, or larger, for these combinations, the emergence of cracking activity of alumina at 400°C becomes understandable. Furthermore, it explains why cracking reactions on alumina "take-off" rather briskly at higher temperatures as is shown, for instance, by the rather steep rate-vs-temperature curve for cumene cracking above 400°C.

The assumption of the existence of *passive Bronsted acids* on alumina surfaces is compatible with the surface structure of alumina. From energy considerations (*8*), it is generally accepted that the outside layer of alumina consists of oxide ions with aluminum ions forming the next lower layer. This alumina surface is highly defective. The presence of anionic defects in the surface oxide layer and the exposed aluminum ions have been discussed by Peri (*7*); the presence of cationic vacancies has been pointed out by Verwey (*9*). Verwey envisioned that γ-alumina has a defective spinel lattice and possesses, on the average, 21⅓ cations and 2⅔ vacancies distributed over 24 definite positions. With this background information, one may assume, parallel to the proposal made for silica-alumina (*10*), that water will interact with the Lewis acid sites, most probably through coordination with an exposed aluminum ion, which is coordination-deficient. Thus

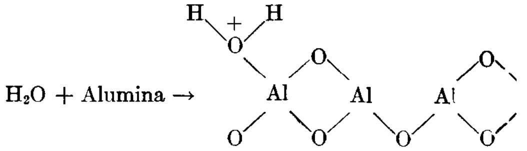

Following this initial coordination, the adsorbed water molecule may ionize, and the resulting hydroxyl group may subsequently locate itself in an anionic vacancy in the oxide layer. In the meanwhile, the proton may drop into a cationic vacancy in the next lower layer. This may be schematically represented as follows.

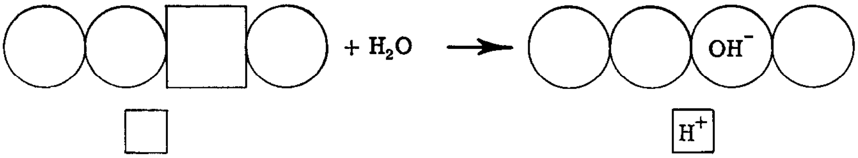

Here, the circles represent the filled lattice sites, while the large square represents an anionic vacancy and the small square, a cationic vacancy. The possibility of protons being trapped in vacancies has previously been pointed out by Dowden (*11*). These protons, trapped in cationic vacancies, are *passive protons*. They are not readily accessible to promote surface reactions unless enough energy has been furnished such that they can first dissociate themselves from the cationic vacancies. The thermal energy corresponding to 400°C where the cracking activity of alumina seems to emerge is 0.06 ev.

It is not necessary that all the *passive protons* be generated from the interaction of water and Lewis acid sites; some of these protons could be inherently present in the lattice structure (*12*).

In connection with the activity of passive Bronsted acids, one more piece of evidence we observed is relevant. Data reported here on hexene cracking are those with liquid feed. When instead of a liquid, a helium stream saturated with hexene vapor was used as feed, a yellowish condensate began to form on the reactor wall near the outlet when the reactor temperature reached 400°C. This suggests that alumina also promotes olefin polymerization at above 400°C.

The passive Bronsted acid interpretation also explained another observed characteristic of alumina which could otherwise be quite puzzling. Although alumina responds positively to most of the acid indicators (*13*), and its acidity can be titrated (*14*), we have found that the acid color on alumina surfaces disappears completely when a trace of water is introduced. Under similar circumstances, the acid color persists on the silica-alumina surfaces. This indicates that on alumina surfaces, Lewis acid sites will react with water to form Bronsted acids but these Bronsted acids, upon their formation, are trapped in the cationic vacancies and become inaccessible to reaction with color indicators.

The inadequacy of Lewis acid sites on the alumina surfaces to promote cracking of unsaturates such as hexene and cumene can now be understood in terms of the carbonium ion mechanism. Denoting the Lewis acid sites by L^+, the cracking of hexene may be, in part, formally represented as follows:

$$CH_3 - CH_2 - CH_2 - CH_2 - CH = CH_2 + L^+$$

$$\rightarrow CH_3 - CH_2 - CH_2 - CH_2 - CH - CH_2L$$

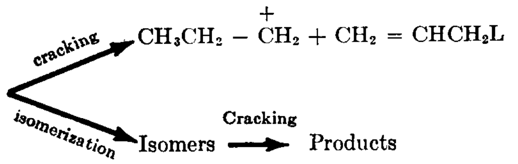

The carbonium ion fragment, generated through β scission, may propagate the cracking through a normal carbonium ion scheme for a while, but sooner or later, a proton will be generated by a reaction such as

$$\text{Carbonium ion} \rightarrow \text{olefin} + H^+$$

This proton may then combine with a cationic vacancy on the surface, and the propagation is stopped. In this way, interaction of olefins with the Lewis acid sites also contributes to the formation of passive Bronsted acids. The other fragment, the olefinic portion of the cracking product ($CH_2 = CHCH_2L$), remains bound to the surface sites. The subsequent desorption of these species and the regeneration of acid sites for reuse are possible only by reaction with protons, e.g.,

$$CH_2 = CHCH_2L + H^+ \rightarrow CH_2 = CHCH_3 + L^+$$

Therefore, it seems that the Lewis acid alone can only contribute to the initial cracking activity of alumina which was indeed observed experimentally (Fig. 4). The sustaining cracking activity of alumina, however, depends on the activity of passive Bronsted acids.

REFERENCES

1. PINES, H., AND HAAG, W. O., *J. Am. Chem. Soc.* **82**, 2471 (1960) and subsequent papers by PINES *et al.*
2. LOBO, P. A., COLDIRON, D. C., VERNON, L. N., AND ASHTON, A. T., *Chem. Eng. Progr.* **58**, 85 (1962).
3. WALL, J., Alcoa Research Laboratory, private communication.
4. VOGE, H. H., AND MAY, W. C., *J. Am. Chem. Soc.* **68**, 550 (1946).
5. HOLM, V. C. F., BAILEY, G. C., AND CLARK, A., *J. Phys. Chem.* **63**, 129 (1959).
6. HANSFORD, R. C., *Ind. Eng. Chem.* **39**, 849 (1947).
7. PERI, J. B., *in* "Actes du Deuxième Congrès International de Catalyse," p. 1333. Èditions Technip, Paris, 1961.
8. DE BOER, J. H., *Industry Chem. Belge* **T21**, 1159 (1956).
9. VERWEY, E. J. W., *J. Chem. Phys.* **3**, 592 (1935).
10. TAMELE, M. W., *Discussions Faraday Soc.* p. 270 (1956).
11. DOWDEN, D. A., *J. Chem. Soc.* p. 242 (1950).
12. HOUBEN, G. M. M., Thesis, Delft University, The Netherlands, 1951.
13. BENESI, H. A., *J. Phys. Chem.* **61**, 970 (1957).
14. HIRSCHLER, A. E., AND SCHNEIDER, A., *J. Chem. Eng. Data* **6**, 313 (1961).